7. Mechanical motor design

Mechanical motor design is as vital as the electromagnetic motor design to build good motors. This comprises questions concerning the
- rotor balancing,
- motor bearing systems,
- cooling and heat transfer,
- mechanical stress of motor parts and their vibration behaviour,
- constructive design of motor parts with respect to insulation co-ordination of electric parts.

7.1 Rotor balancing

The rotating rotor body is usually not an ideal mechanical system with the centre of gravity located on the rotational axis, but under real conditions centre of gravity is dislocated from rotational axis by a certain displacement e_S. Thus **centrifugal force** F of rotor mass m_r

$$F = m_r \cdot e_S \cdot \Omega_m^2 \tag{7.1-1}$$

at rotational angular frequency

$$\Omega_m = 2\pi \cdot n \quad , \quad n\text{: rotational speed} \tag{7.1-2}$$

will occur as radial force in direction of dislocation of centre of gravity from rotor axis, trying to bend the elastic rotor and acting as additional forces at the rotor bearings. As direction of this force rotates with rotational speed, it may excite mechanical vibrations of the whole motor with frequency $f = n$, which – when hitting natural vibration frequency of motor system – causes resonance with increased vibration amplitude. So, **imbalance** may lead to
- increased bearing stress,
- additional rotor loading and
- increased machine vibrations.

In order to quantify imbalance, usually the real system with elastic rotor and elastic bearings is modelled by step-wise by **idealized models**. All effects of rotor vibration are included in the **theory of rotor dynamics**, which is a mathematical discipline of theoretical mechanics.

rotor model	*rotor*	*bearings*
rigid rotor model	rotor body shows no deformation under force load (= geometry does not change shape under force load)	rigid bearings show no deformation under force load
elastic rotor model	rotor body is deformed under force load (= *Young´*s modulus of elasticity E of rotor material is not infinite)	rigid bearings
elastic bearing model	elastic rotor body	bearing geometry is deformed under force load (deformation is ruled by *Young´*s modulus of elasticity E of bearing material and end shields)

Table 7.1-1: Different mathematical models for rotor system (= rotor body and bearings)

Elastic rotor is bending under radial force load, thus acting like a spring with a natural bending frequency f_{b1}. If exciting frequency $f = n$ stays below 70% of f_{b1}, no resonance effect will occur and rotor bending deformation will usually be small, and therefore is neglected. Thus with **maximum speed n_{max} below** $0.7 \cdot f_{b1}$, usually the rigid rotor model is used for calculation of mechanical vibration. Please note, that in addition to mechanical imbalance also

"unbalanced magnetic pull" may be active, which in case of 2-pole machines with eccentric rotor, as explained in Chapter 5, may excite radial forces with $f = 2n$. Then of course limit for rigid rotor model is $n_{max} \leq 0.35 \cdot f_{b1}$.

Calculation of rotor dynamics and technique of balancing rotors is today fine art, which is taught in special lectures. International standardization ISO1925, ISO1940 and ISO5460 and the national *German* guide line "VDI-Richtlinie 2060" apply. Here, only the basics will be given in short to get an overview.

7.1.1 Imbalance of rigid rotor bodies

a) Disc rotor:
We assume the rotor body to be rigid as well as the bearings. Thermal influence on rotor, which leads e.g. also to axial rotor expansion (*z*-direction in Fig. 7.1.1-1), which may be different from thermal expansion of stator housing, is coped with one of the two bearings being a loose bearing. That means, that the rotor and this bearing may move in axial direction (usually axial movement is well below 1 mm) under expansion, whereas the other bearing is fixed in axial direction. The most simple model is a **disc-like rotor** (thickness l_{Fe} much smaller than diameter d_{ra} and bearing distance L) with rotor mass m_r, mounted on an infinite stiff, but very thin shaft (shaft length between bearing is bearing distance L) (Fig. 7.1.1-1). For simplification we assume disc to be centred between the bearings.

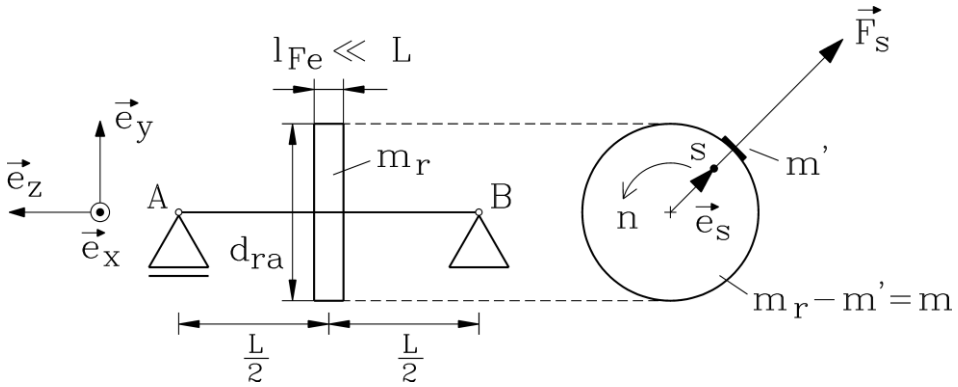

Fig. 7.1.1-1: Rigid body disc rotor on stiff shaft with centre of gravity *S* dislocated from rotational axis by distance e_S (left: loose bearing A, right: fixed bearing B).

Dislocation e_S of centre of gravity *S* from rotational axis, which is centred at geometrical centre of disc, is e.g. given by an additional mass *m´* at radius $d_{ra}/2$, whereas the mass $m_r - m'$ is evenly distributed on the disc. Thus centre of gravity of mass $m_r - m'$ is located on rotational axis. At standstill gravity will drag additional mass *m´* down right below rotational axis, thus turning the disc in that position, so one can recognize the imbalance also at standstill, hence calling it **static imbalance**. The maximum torque exerted by gravity on the disc at stand still occurs at disc position where additional mass is in horizontal plane:

$$M = m' \cdot g \cdot d_{ra}/2 = m_r \cdot g \cdot e_S \qquad \Rightarrow \quad e_S = (m'/m_r) \cdot (d_{ra}/2) \tag{7.1.1-1}$$

Denoting the displacement as a vector, directed from centre of rotation to centre of gravity, we get under rotation the radial centrifugal force vector, which defines the **static imbalance vector** $\vec{U}_S$, which is NOT a force:

$$\boxed{\vec{F}_S = m_r \cdot \vec{e}_S \cdot \Omega_m^2 \qquad \Rightarrow \quad \vec{U}_S = \frac{\vec{F}_S}{\Omega_m^2} = m_r \cdot \vec{e}_S} \tag{7.1.1-2}$$

Conclusions:
Static imbalance U_S is the proportional coefficient between square of angular mechanical frequency and centrifugal force. It is independent of speed.

Example 7.1.1-1:
Rotor mass m_r = 60 kg, rotor outer diameter d_{ra} = 200 mm, m' = 2 g,

$$e_S = (m'/m_r) \cdot (d_{ra}/2) = (2/60000) \cdot (0.2/2) = \underline{\underline{3.33}}\,\mu\text{m}$$

$$U_S = m_r \cdot e_S = 60 \cdot 3.33 \cdot 10^{-6} = \underline{\underline{200}}\,\text{g·mm}$$

Centrifugal force at n = 2000/min:

$$F_S = m_r \cdot e_S \cdot \Omega_m^2 = 60 \cdot 3.33 \cdot 10^{-6} \cdot (2\pi \cdot 2000/60)^2 = \underline{\underline{8.8}}\,\text{N}$$

Note: Gravity force of rotor is $m_r \cdot g = 60 \cdot 9.81 = 589\,\text{N}$. Already at a small displacement of centre of gravity by 3.3 μm, a centrifugal force of 8.8/589 = 1.5% of rotor gravity force occurs at 2000/min. At 4000/min centrifugal force is already 6% of gravity force. As already such small displacements e_S cause considerable centrifugal forces, it is easily understood, that it is practically impossible to build rotors with no imbalance. A balancing process is always necessary.

The rotating force $\vec{F}_S = F_S \cdot \vec{e}_x \cdot \cos(\Omega_m t) + F_S \cdot \vec{e}_y \cdot \sin(\Omega_m t)$ may be decomposed into an *x*- and *y*-component according to Fig. 7.1.1-1. As disc is centred between bearings, the load bearing forces in A and B are identical due to symmetry: In vertical direction (*y*-direction) gravity load and imbalance load occur, whereas in horizontal direction (*x*-direction) only imbalance is acting.

$$\begin{aligned} \vec{F}_{A,x} &= \vec{F}_{B,x} = F_S/2 \cdot \cos(\Omega_m t) \\ \vec{F}_{A,y} &= \vec{F}_{B,y} = m_r \cdot g/2 + F_S/2 \cdot \sin(\Omega_m t) \end{aligned} \tag{7.1.1-3}$$

$$\begin{aligned} \vec{F}_{A,x\sim} &= \vec{F}_{B,x\sim} = U_S \cdot \Omega_m^2/2 \cdot \cos(\Omega_m t) \\ \vec{F}_{A,y\sim} &= \vec{F}_{B,y\sim} = U_S \cdot \Omega_m^2/2 \cdot \sin(\Omega_m t) \end{aligned} \tag{7.1.1-4}$$

Conclusions:
Due to static imbalance an additional oscillating bearing force occurs. With the square of increasing speed this oscillating component of the bearing load increases due to static imbalance, with oscillation frequency being rotational frequency. In both bearings this additional bearing force is IN PHASE (common mode force).

b) Finite length rotor:
Due to rotor iron stack length l_{Fe} electric motor rotors are usually not disc-like (Fig. 7.1.1-2). Let us assume an ideal cylindrical rotor with cylinder length l_{Fe}, being placed centred between bearings A and B. Ideal cylinder has its centre of gravity on cylinder axis, which is here also rotational axis. If two additional masses m'' are placed on the cylinder ends in opposite radial position at cylinder circumference, they will not shift centre of gravity from rotational axis. So at stand still rotor will NOT move under gravitational force. But if rotor is rotating, on each of the two masses a centrifugal force F'' with opposite direction will occur

$$F'' = m'' \cdot (d_{ra}/2) \cdot \Omega_m^2 \quad , \tag{7.1.1-5}$$

resulting due to this force pair in an additional torque

$$\boxed{M'' = m'' \cdot (d_{ra}/2) \cdot \Omega_m^2 \cdot l_{Fe} \quad \Rightarrow \quad M_U = \frac{M''}{\Omega_m^2} = \frac{m'' \cdot d_{ra} \cdot l_{Fe}}{2}} \quad . \tag{7.1.1-6}$$

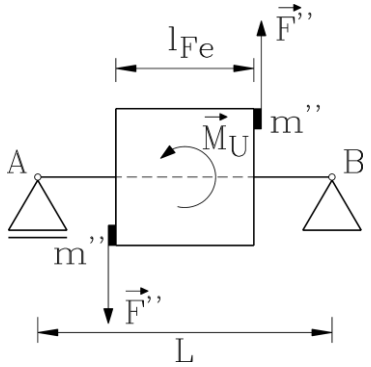

Fig. 7.1.1-2: Rigid body cylindrical rotor with centre of gravity *S* located on rotational axis, but uneven distributed mass along rotor axis, represented here by two masses *m*" , which lead to imbalance torque *M*", when rotor is rotating.

As the effect of this mass arrangement is only active at rotor rotation, whereas at stand still no effect is visible, we call this a **dynamic imbalance** M_U, which is defined as torque per square of rotational angular frequency. Note, that no total centrifugal force occurs, as the two force components are opposite, cancelling each other: $F_S = F'' - F'' = 0$. The additional torque M'' leads to reaction forces ΔF in the two bearings as a force pair with opposite direction of ΔF in the two bearings, which counter-balance this torque:

$$M'' = F'' \cdot l_{Fe} = \Delta F \cdot L \qquad \Rightarrow \Delta F = (l_{Fe}/L) \cdot F'' \tag{7.1.1-7}$$

$$\begin{aligned} \vec{F}_{A,x\sim} &= -\vec{F}_{B,x\sim} = (M_U/L) \cdot \Omega_m^2 \cdot \cos(\Omega_m t) \\ \vec{F}_{A,y\sim} &= -\vec{F}_{B,y\sim} = (M_U/L) \cdot \Omega_m^2 \cdot \sin(\Omega_m t) \end{aligned} \tag{7.1.1-8}$$

Conclusions:
Dynamic imbalance M_U is the proportional coefficient between square of angular mechanical frequency and imbalance torque. It is independent of speed. It leads to additional oscillating bearing forces with opposite sign in both bearings (= 180° phase shift = differential mode force), again with oscillation frequency equal to rotational speed.

In real rotors both effects, static imbalance due to dislocation of centre of gravity from rotational axis, and dynamic imbalance due to uneven mass distribution along rotor axis, occur. Thus bearing oscillating force are containing a **common-mode component** due to static imbalance and a **differential mode component** due to dynamic imbalance.

In Fig. 7.1.1-3 examples for imbalance are given:
a) Disc rotor with static imbalance: The centre of gravity *S* turns at standstill beneath rotational axis under the influence of gravity. Thus effect of static imbalance can be experienced already at stand still (at static conditions).

b) Dynamic imbalance if disc rotor: Inertia axis of disc rotor (which is geometric of disc, if disc mass is homogenous distributed) is not aligned with rotor axis. Thus centre of gravity of upper and lower half disc is displaced axially by Δz. Under rotation, the centrifugal forces F'' lead to imbalance torque $M'' = F'' \cdot \Delta z$.

c) Superposition of static and dynamic imbalance: A cylindrical rotor with inertia axis unaligned with rotational axis in that way, that also the centre of gravity *S*, located on inertia axis, is dislocated from rotational axis.

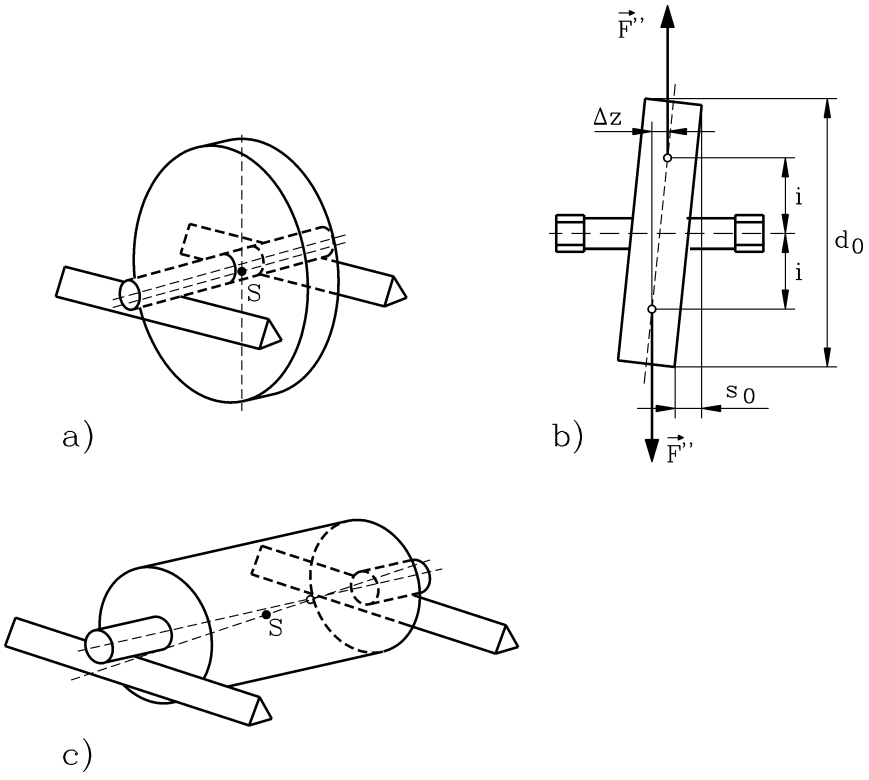

Fig. 7.1.1-3: Examples for rigid body imbalance: a) static imbalance, b) dynamic imbalance, c) static and dynamic imbalance

If we decompose the cylindrical rotor of Fig. 7.1.1-3c by thought into cylindrical thin disc slices ($l_{Fe,disc} \to 0$), each of these rotor discs will be thin enough to produce no imbalance torque ($M''_{disc} \sim l_{Fe,disc} \to 0$). Each disc has therefore only static imbalance of different amplitude and direction. In Fig. 7.1.1-4 this is shown for example for rotor decomposed in 3 disc slices. The static imbalance e.g. of disc 3 U_3 leads to centrifugal force F_{S3} at speed *n*. When disc 3 is placed at co-ordinate z_3, we get the reaction forces in the bearings A = L (left) and B = R (right):

force equilibrium: $F_{S3} = F_{L3} + F_{R3}$, torque equilibrium: $M_{S3} = F_{S3} \cdot z_3 = F_{R3} \cdot L$, yielding to

$$F_{L3} = F_{S3} \cdot \frac{L - z_3}{L}, \quad F_{R3} = F_{S3} \cdot \frac{z_3}{L} \qquad . \tag{7.1.1-9}$$

Superposition of $\vec{F}_L = \vec{F}_{L1} + \vec{F}_{L2} + \vec{F}_{L3}$, $\vec{F}_R = \vec{F}_{R1} + \vec{F}_{R2} + \vec{F}_{R3}$ leads to resulting bearing forces $\vec{F}_L, \vec{F}_R$, corresponding with $\vec{U}_L = \vec{F}_L / \Omega_m^2, \vec{U}_R = \vec{F}_R / \Omega_m^2$ in Fig. 7.1.1-4. Bearing forces and corresponding imbalance may ALWAYS be decomposed in **common mode** (S: *symmetrical*, resultant static component) and **differential mode component** (A: *anti-symmetrical*, resultant dynamic component).

$$\vec{F}_L = \vec{F}_S + \vec{F}_A, \quad \vec{F}_R = \vec{F}_S - \vec{F}_A \quad \Rightarrow \quad \vec{F}_S = (\vec{F}_S + \vec{F}_S)/2, \quad \vec{F}_A = (\vec{F}_L - \vec{F}_R)/2 \qquad (7.1.1\text{-}10)$$

Conclusions:

In general case additional bearing force in left and right bearing are not directed in the same direction, but in arbitrary one. Nevertheless each bearing force may always be written as a sum of common and a differential mode component. This each rigid rotor imbalance is given as a superposition of a total static and dynamic imbalance.

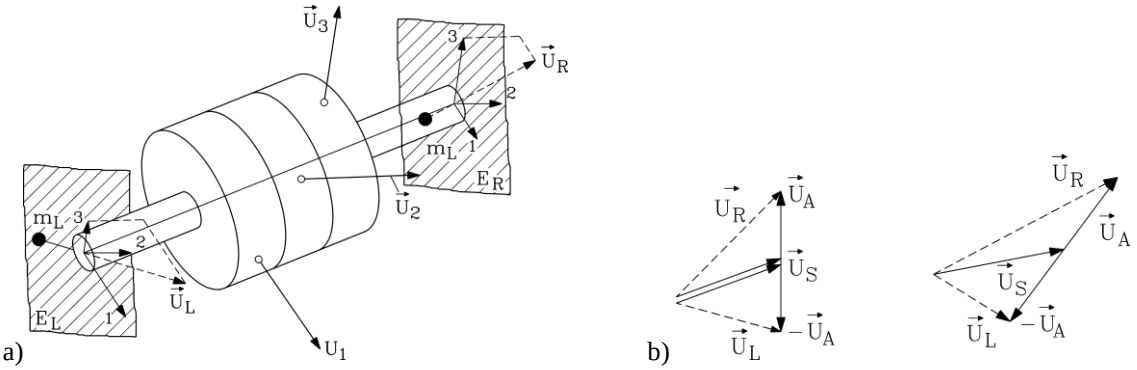

Fig. 7.1.1-4: a) A cylindrical rotor with static and dynamic imbalance is decomposed into three disc slices. For each disc slice the dynamic imbalance may be neglected. So the total imbalance is given by the sum of the static imbalances of each disc. Its components in the bearing planes (L: left, R: right) are summed up as vectors for total bearing reaction. b) The bearing reaction imbalance may be decomposed into a static and dynamic component by taking common mode (symmetrical: S) and differential mode (anti-symmetrical: A) component. This decomposition is always possible for any arbitrary imbalance component in the R and L bearing plane.

7.1.2 Balancing equation for rigid rotor bodies

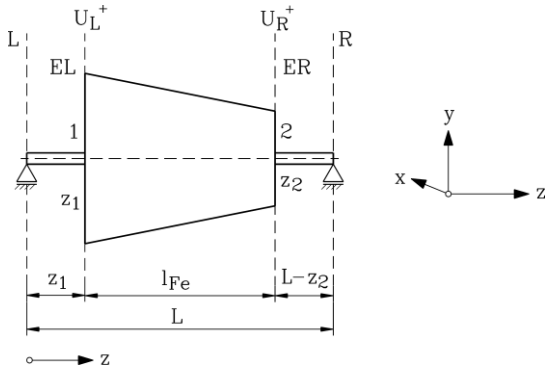

Fig. 7.1.2-1: Balancing of rotor with static and dynamic imbalance by two additional masses fixed in the planes EL and ER to compensate the additional imbalance bearing forces

If two additional masses m_L and m_R would be added in the bearings opposite to the bearing additional forces at a certain distance (Fig. 7.1.1-4), their centrifugal forces would cancel the bearing additional forces. This is the basic idea of balancing a rotor by additional masses. As in the bearings there is no space for additional masses, the idea is to use additional balancing planes at the co-ordinates z_1 and z_2, where the additional masses are fixed. In many cases the end planes of the rotor body itself are used as these balancing planes (Fig. 7.1.2-1). By fixing the two balancing masses m_1, m_2 at the radii r_1, r_2 in those two balancing planes EL and ER ($\vec{U}_1 = m_1\vec{r}_1, \vec{U}_2 = m_2\vec{r}_2$), their additional centrifugal forces $\vec{F}_1 = \vec{U}_1\Omega_m^2, \vec{F}_2 = \vec{U}_2\Omega_m^2$ must be such, that their reaction forces $\vec{F}_L^+, \vec{F}_R^+$ in the bearings compensate the imbalance bearing forces $\vec{F}_L, \vec{F}_R$ which are caused by the original rotor imbalance (Fig. 7.1.1-4). Assuming for simplification F_L, F_R directed in the same plane, we get

force equilibrium: $F_L^+ + F_R^+ = F_1 + F_2$, torque equilibrium: $F_R^+ \cdot L = F_1 \cdot z_1 + F_2 \cdot z_2$, thus

$$F_1 = F_L^+ \cdot \frac{z_2}{z_2 - z_1} - F_R^+ \cdot \frac{L - z_2}{z_2 - z_1}$$
$$F_2 = -F_L^+ \cdot \frac{z_1}{z_2 - z_1} + F_R^+ \cdot \frac{L - z_1}{z_2 - z_1} \qquad (7.1.2\text{-}1)$$

With $F_L^+ = -F_L = -U_L \Omega_m^2$, $F_R^+ = -F_R = -U_R \Omega_m^2$ we get for the balancing masses the **balance equations**

$$\boxed{U_1 = m_1 r_1 = \frac{-U_L + U_R \cdot (L / z_2 - 1)}{1 - z_1 / z_2}}$$
$$\boxed{U_2 = m_2 r_2 = \frac{U_L \cdot (z_1 / z_2) - U_R \cdot (L / z_2 - z_1 / z_2)}{1 - z_1 / z_2}} \qquad (7.1.2\text{-}2)$$

Example 7.1.2-1:
Medium sized electric motor of 75 kW, 1500/min, rotor mass m_r = 60 kg, rotor outer diameter 200 mm, balancing in two planes at $L / z_2 = 3/2$, $z_1 / z_2 = 1/2$, balancing radii:
$r_1 = r_2 = d_{ra} / 2 = 100\,\text{mm}$.
Measured imbalance bearing forces at 500 /min: $F_L = 1.6\,\text{N}$, $F_R = 1.0\,\text{N}$. We assume force direction in both bearings to be the same.
How big must be the compensating balancing masses m_1, m_2 to compensate completely rotor imbalance ?

$$U_L = F_L / \Omega_m^2 = 1.6 / (2\pi(500/60))^2 = 583.6\,\text{g·mm}$$
$$U_R = F_R / \Omega_m^2 = 1.0 / (2\pi(500/60))^2 = 364.8\,\text{g·mm}$$
$$m_1 = \frac{-U_L + U_R \cdot (L / z_2 - 1)}{1 - z_1 / z_2} \cdot \frac{1}{r_1} = \frac{-583.6 + 364.8 \cdot (3/2 - 1)}{1 - 1/2} \cdot \frac{1}{100} = \underline{\underline{-8g}}$$
$$m_2 = \frac{U_L \cdot (z_1 / z_2) - U_R \cdot (L / z_2 - z_1 / z_2)}{1 - z_1 / z_2} \cdot \frac{1}{r_2} = \frac{583.6 \cdot (1/2) - 364.8 \cdot (3/2 - 1/2)}{1 - 1/2} \cdot \frac{1}{100} = \underline{\underline{-1.46g}}$$

Balancing masses are 8 g and 1.5 g, which – due to negative sign – must be fixed opposite to direction of measured bearing forces, or this amount of mass must be removed from the rotor.

Conclusions:
From balancing equations one concludes that balancing masses for given imbalance are smaller, if the fixing radii r_1, r_2 for these masses are big, so usually outer rotor diameter is chosen. They are also small, if the distance between the two balancing planes z_2 - z_1 is big.

7.1.3 Balancing of rigid rotors

Rotor is put on to measuring bearings in the balancing machine (Fig. 7.1.3-2) and is driven by a small motor on to balancing speed *n*. The measuring bearings have a certain elasticity, which may be expressed by the stiffness c_B. Due to imbalance the rotor generates *n*-frequent force oscillation $\hat{F} \cdot \cos(\Omega_m t)$ in the bearings, which vibrate. In horizontal plane *x* no gravity force is acting, so we get

$$m_r \cdot \ddot{x} + c_B \cdot x = \hat{F} \cdot \cos(\Omega_m t) \tag{7.1.3-1}$$

Solution of this second order linear differential equation with constant coefficients is

$$x(t) = \hat{X} \cdot \cos(\Omega_m t) \quad , \quad \hat{X} = \frac{\hat{F}}{c_B - \Omega_m^2 \cdot m_r} \quad , \quad \Omega_m = 2\pi \cdot n \qquad . \tag{7.1.3-2}$$

At resonance frequency $n = f_B$ amplitude of this (here assumed) loss-free oscillation vibration amplitude tends to infinite, thus denominator is zero, yielding for f_B

$$c_B - \Omega_m^2 \cdot m_r = 0 \quad \Rightarrow \quad n = f_B = \frac{1}{2\pi} \cdot \sqrt{\frac{c_B}{m_r}} \qquad . \tag{7.1.3-3}$$

If rotor speed n is operated well below or well above resonance frequency, resonance is avoided and we get

$$\begin{aligned} \underline{n << f_B}: \quad & \hat{X} \approx \frac{\hat{F}}{c_B} \quad \Rightarrow \quad \hat{F} = \hat{X} \cdot c_B = U \cdot \Omega_m^2 \\ \underline{n >> f_B}: \quad & \hat{X} \approx \frac{\hat{F}}{-\Omega_m^2 \cdot m_r} = -\frac{U}{m_r} \end{aligned} \tag{7.1.3-4}$$

In order to operate at the same speed with $n << f_B$, one has to build stiff bearings with high stiffness c_B as shown in Fig. 7.1.3-1a. A pressure sensor (e.g. piezo-electric sensor) between a stiff basement construction and the V-shaped bearing directly measures the horizontal force amplitude $\hat{F} = U \cdot \Omega_m^2$, which is directly proportional to imbalance (**stiff measuring bearing**). If operation should be done at $n >> f_B$ for the same speed, one has to build "soft" bearings with low stiffness c_B as shown in Fig. 7.1.3-1b. The V-shaped bearing is fixed by long springs to the basement construction. The longer the spring, the lower is the value c_B. An e.g. inductive position sensors is directly measuring the horizontal movement of the measuring bearing $\hat{X} = -U / m_r$, which is directly proportional to imbalance U (**low stiffness measuring bearing**). Both methods are used nowadays to measure the imbalance.

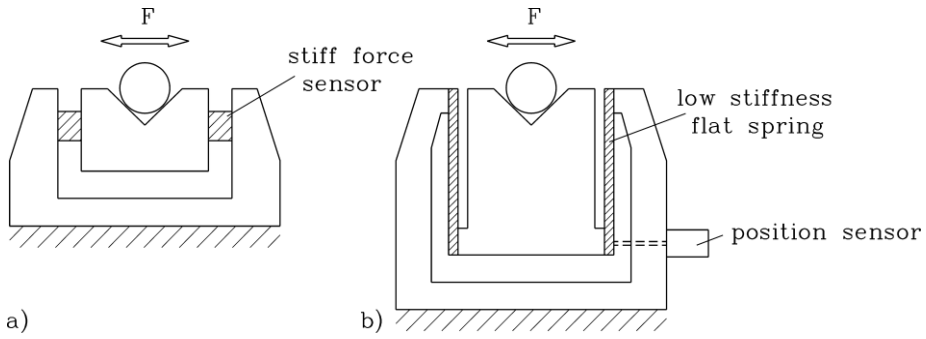

Fig. 7.1.3-1: Measuring rotor imbalance a) with bearing force measurement, b) bearing position measurement

Measurement signal of bearing force $F_R(t)$, $F_L(t)$ or bearing position $s_R(t)$, $s_L(t)$ contains not only rotational frequency, but due to other excitations like the balls of the bearings additional harmonics and also some noise due to EMI (Fig. 7.1.3-2). So signal is filtered with low pass

filter, then only getting the *n*-frequent signals $R(t), L(t)$, which have same frequency, but different amplitude and phase shift. If the signals are taken as phasors, rotating with Ω_m in the complex plane according to

$$\begin{aligned} \underline{\hat{L}} = \hat{L} \cdot e^{j\varphi_L} \quad &\Leftrightarrow \quad L(t) = \hat{L} \cdot \cos(\Omega_m t + \varphi_L) = \mathrm{Re}\left\{\underline{\hat{L}} \cdot e^{j\Omega_m t}\right\} \\ \underline{\hat{R}} = \hat{R} \cdot e^{j\varphi_R} \quad &\Leftrightarrow \quad R(t) = \hat{R} \cdot \cos(\Omega_m t + \varphi_R) \end{aligned} \quad , \qquad (7.1.3\text{-}5)$$

one can take them directly as the imbalance vectors $\vec{U}_L, \vec{U}_R$, which are used as input for the balancing equation (7.1.2-2). With the balancing masses m_1, m_2 calculated from (7.1.2-2), these masses are fixed to the rotor and measurement of bearing forces or position is repeated.

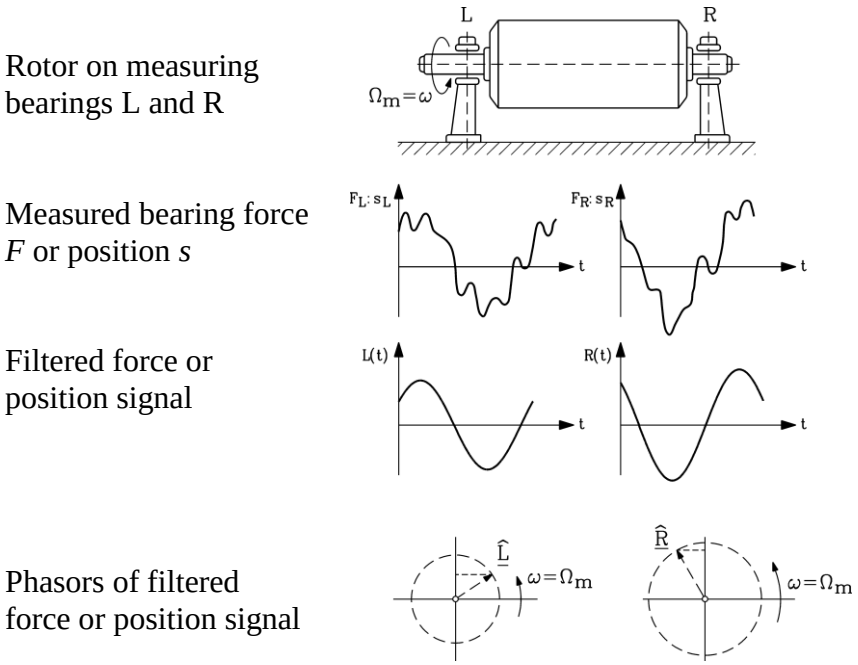

Fig. 7.1.3-2: Measuring of rotor imbalance by deducing resultant imbalance in the bearings

If balancing is ideal, now no *n*-frequent bearing forces should occur any longer. In reality of course still some small imbalance is left. This residual imbalance must stay below certain limits, whereby these limits are defined – depending on the purpose of the rotor – by standard ISO 1940. This residual imbalance is not given as imbalance value, but as **circumference speed of centre of gravity**

$$G = \Omega_m \cdot e_S \quad . \qquad (7.1.3\text{-}6)$$

In ideal case with centre of gravity on rotational axis $G = \Omega_m \cdot e_S = \Omega_m \cdot 0 = 0$, so G can also be taken as measure for residual imbalance.

Example 7.1.3-1:
Limit of residual imbalance according to ISO 1940 for electric motor, 2000/min, 100 kW, rotor mass 100 kg.
Table 7.1.3-1: $G = 2.5 mm/s \quad \Rightarrow \quad e = G/\Omega_m = 0.0025/(2\pi \cdot 2000/60) = 11.9 \mu\mathrm{m}$

Residual imbalance: $U = 11.9 \cdot 10^{-6} \cdot 100 = \underline{\underline{1194}}\,\mathrm{g \cdot mm}$

	$\Omega_m \cdot e_S$	*Examples*
	mm/s	
G 4000	4000	Slow turning big *Diesel* engines for ships
G 1600	1600	Big two stroke combustion engines
G 630	630	Big four stroke combustion engines
G 250	250	Fast turning four stroke piston engines
G 100	100	Combustion engines for cars and locomotives
G 40	40	Wheel sets for cars
G 16	16	Cardan transmission shafts
G 6.3	6.3	Fans, pump rotors, standard electric motor rotors
G 2.5	2.5	Rotors of steam and gas turbines, big electric generators, high speed electric motors, turbo prop for air craft
G 1	1	Ultra high speed small motors, grinding spindle drives
G 0.4	0.4	Gyroscopic rotors, special high speed grinding spindle drives

Table 7.1.3-1: Limits for residual imbalance according to ISO 1940

Methods for balancing:
With wound rotors of small up to medium sized motors of DC machines, universal motors, wound rotor induction machines the balancing masses are a special fast-hardening cement, put into the winding overhangs of the rotor winding.
Cage induction rotors often have special cylindrical noses integrated into the aluminium end rings of the cage. On these noses metal rings are fixed as balancing masses.
For high speed machines these noses might cause additional friction in air, therefore often some cage mass is cut off (**" negative masse balancing"**).
Bigger machines get special additional discs on the rotor, where the balancing masses are fixed.

7.1.4 Balancing of complete motor system

After mounting the rotor into the stator housing and the end-shields, the additional imbalance might be induced by inaccuracy of bearing seats in the end shields. For high speed motors or motors for very low vibration therefore additional balancing is necessary e.g. by cutting of some mass from rotor shaft end or by cutting off some mass of special rotor discs. Thus **balancing of the complete motor** is done. This has to be done at cold motor, but has to be repeated at hot motor, because due to uneven thermal expansion of rotor additional imbalance might occur (**thermally induced imbalance**). For example, the iron sheets of rotor iron stack usually do not have exactly parallel sides, so thickness varies a little bit along the sheet plane. If all sheets are stacked on the rotor shaft with bigger thickness on one side, thermal expansion there is bigger, causing the rotor to bend, when hot. Thus centre of gravity is displaced, causing imbalance. By stacking the rotor with the rotor sheets shifted by 90° each, this effect is equalized, thus avoiding this reason for thermal imbalance.

But how to check the status of imbalance at the completed motor ?
Motor is put on an elastic test bed, e.g. beneath motor feet thick rubber pads are put (Fig. 7.1.4-1a). Another possibility is to hang the motor into springs. This method is of course only possible for smaller motors (Fig. 7.1.4-1b).

Vibration measurement in radial perpendicular direction (*x*, *y*-co-ordinate) at the bearing location (= end shields) and in axial direction (*z*-co-ordinate) is done with respect to rotational

frequency $f = n$, e.g. by measuring vibration velocity v or acceleration a. If motor housing surface position in horizontal direction is x, we get

$$x(t) = \hat{X} \cdot \cos(\omega t), \quad v(t) = \dot{x}(t) = -\omega \hat{X} \cdot \sin(\omega t), \quad a(t) = \ddot{x}(t) = -\omega^2 \hat{X} \cdot \cos(\omega t) \qquad (7.1.4\text{-}1)$$

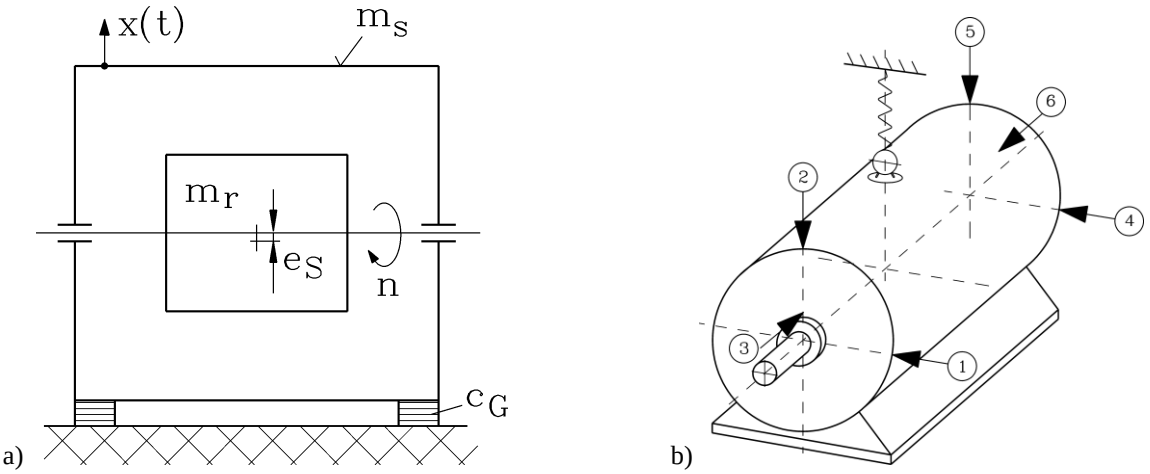

Fig. 7.1.4-1: Vibration measurement for completed motor: a) motor put on rubber pads, b) motor hung in springs

Motor with mass m, consisting of stator mass m_s and rotor mass m_r is put on rubber pads or hung in springs (with spring or pad stiffness c_G). Motor winding is connected to inverter to drive rotor at no-load with different speed n. Rotor imbalance leads to oscillating bearing forces F, which also excite the stator housing to vibrate. Vibration $x(t)$ of stator housing is measured with respect to rotational frequency. We assume static imbalance U_S, getting the x-component of centrifugal force

$$F_S = m_r \cdot e_S \cdot \Omega_m^2 \quad \Rightarrow \quad F_x(t) = F_S \cdot \cos(\Omega_m t) \qquad (7.1.4\text{-}2)$$

for exciting the vibration of the whole motor mass in x-direction:

$$(m_s + m_r) \cdot \ddot{x} + c_G \cdot x = F_S \cdot \cos(\Omega_m t) \quad . \qquad (7.1.4\text{-}3)$$

Due to the low stiffness c_G the resonance frequency f_G is much lower than rated speed. Solution of this linear second order differential equation is according to (7.1.3-2)

$$x(t) = \hat{X} \cdot \cos(\Omega_m t) \quad , \quad \hat{X} = \frac{F_S}{c_G - \Omega_m^2 \cdot m_{mot}} \quad , \quad f_G = \frac{1}{2\pi} \cdot \sqrt{\frac{c_G}{m_{mot}}} \quad . \qquad (7.1.4\text{-}4)$$

Due to the low stiffness c_G the resonance frequency f_G is much lower than rated speed.

$$\underline{n >> f_G}: \quad \hat{X} \approx \frac{F_S}{-\Omega_m^2 \cdot m_{mot}} = -\frac{U_S}{m_{mot}} \quad . \qquad (7.1.4\text{-}5)$$

$$v(t) = \dot{x}(t) = \frac{U_S}{m_{mot}} \cdot \Omega_m \cdot \sin(\Omega_m t) \quad \Rightarrow \quad \hat{v} = \frac{m_r}{m_s + m_r} \cdot e_S \cdot \Omega_m \qquad (7.1.4\text{-}6)$$

Conclusions:
Vibration velocity rises linear with speed, its inclination being directly proportional to imbalance itself. Thus it is possible by elastic mounting of motor to get access to status of imbalance by vibration measurement.

Vibration velocity is directly proportional to circumference velocity of centre of gravity:

$$\hat{v} = \frac{m_r}{m_s + m_r} \cdot e_S \cdot \Omega_m = \frac{m_r}{m_s + m_r} \cdot G \qquad (7.1.4\text{-}7)$$

The imbalance limit G is connected to the r.m.s. limit of vibration velocity by

$$v_{r.m.s} = \frac{m_r}{m_s + m_r} \cdot \frac{G}{\sqrt{2}} \quad . \qquad (7.1.4\text{-}8)$$

Example 7.1.4-1:
With a mass ratio $m_r / m_{mot} = 1/3$ and G = 6.3 mm/s a typical value for r.m.s. vibration velocity limit is $v_{r.m.s} = \frac{1}{3} \cdot \frac{6.3}{\sqrt{2}} = \underline{\underline{1.5}}$ mm/s.

For balancing complete motor system in ISO2373 limits $v_{r.m.s}$ are given, which according to (7.1.4-6) rise with speed. Depending on increased performance of drive system, which is defined by application such as motors for tooling machines, **different vibration levels** are given:
N: normal use (standard),
R, S, SR: decreased vibration level is given by levels R, S and SR (Fig. 7.1.4-2).
These values are given of course not for extremely big motors, as for them it is difficult to put them **on elastic mounting** (Fig. 7.1.4-1) for measurement. Values are defined for AC- and DC-machines with frame size 80 mm to 400 mm (shaft height), corresponding with rated power 0.5 kW up to 450 kW at 1500/min. Vibration levels are defined in IEC34-14 and more detailed in ISO2373.

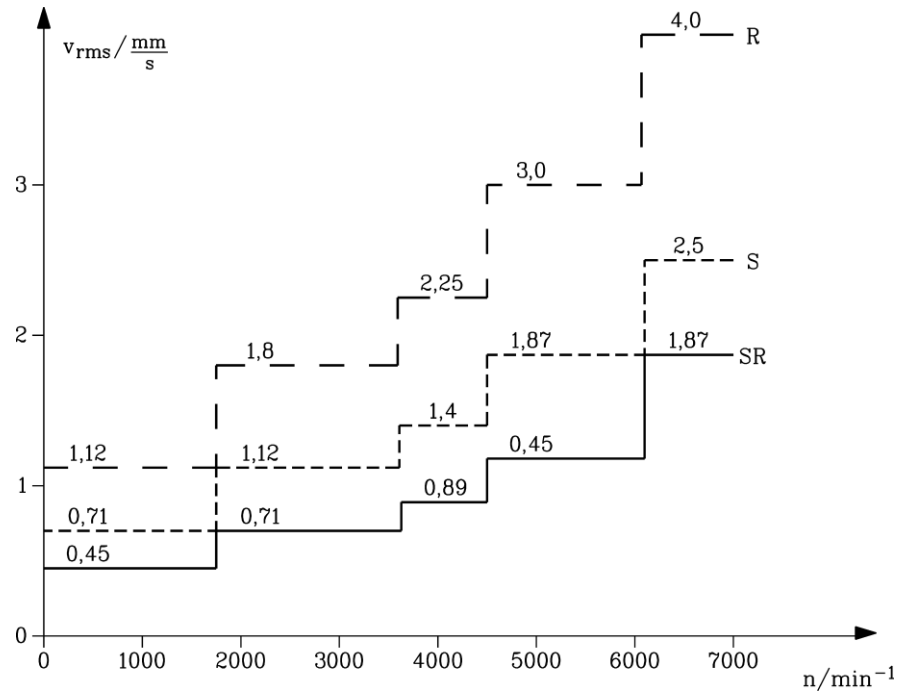

Fig. 7.1.4-2: Vibration levels (r.m.s. vibration velocity), depending on maximum speed of motor, according to ISO2373, for motor size 160 mm to 180 mm

Above frame size 400 mm the motors are too big to be measured on elastic mounting. Therefore only limits of values $v_{r.m.s.}$ for **stiff mounting** are given. In that case machine and

machine bed, where machine is mounted, are coupled, so vibration of machine causes also the bed to vibrate. This measurement method therefore does not allow access to the vibration behaviour of the machine itself, but only of the whole drive system with machine bed. So measurement values may be quite different, when compared with measurement on elastic mounting.

Example 7.1.4-2:
Limits of r.m.s. vibration level according to ISO2372 for frame size 160 mm to 180 mm:
Level N: 2.8 mm/s for variable speed drives with maximum speed 600/min ... 3600/min
Levels R, S, SR are depicted in Fig. 7.1.4-2 for extended speed range up to 7000/min.

7.1.5 Elastic rotor system - Vibrations of rotors

The rotor system is constituted by the rotor body and the bearing system, which comprises the bearings and the end shields or bearing seats. Elasticity of the rotor shaft and of the bearing system leads to natural vibrations of the rotor system, which makes it impossible to balance the rotor only in two balancing planes, as it is possible for rigid rotor body system.

a) Influence of elastic bearings :

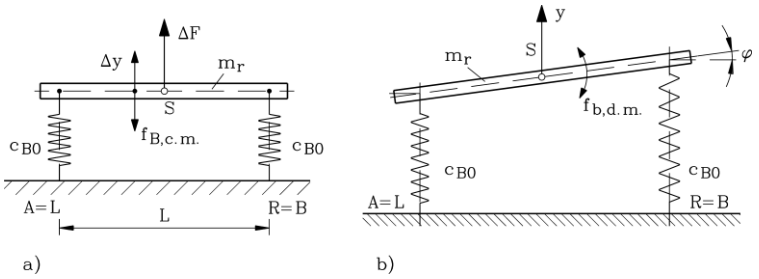

Fig. 7.1.5-1: Rigid body vibration on elastic bearings: a) common mode vibration (c.m.), b) differential mode vibration (d.m.)

The bearing stiffness of ball or roller bearings is much higher than the stiffness of the rotor body. But in case of magnetic bearings, oil sleeve bearings or air bearings the bearing stiffness is smaller. So, if a rigid rotor body is placed on elastic bearings, these bearings may be described by the bearing stiffness c_B (Fig. 7.1.5-1). We assume identical bearings, so equivalent spring systems for left and right bearing are identical: $c_{BL} = c_{BR} = c_{B0}$, yielding for bearing deformation e.g. in vertical direction Δy along with vertical force per bearing $\Delta F_{BL} = \Delta F_{BR} = \Delta F_B$:

$$\Delta F_B = c_{B0} \cdot \Delta y \quad . \tag{7.1.5-1}$$

If both bearings vibrate IN PHASE (common mode vibration) e.g. in vertical direction, the rotor body is also oscillating vertically (Fig. 7.1.5-1a). As both bearing springs act mechanically in parallel, both bearing forces add for the SAME vertical deformation, leading to resulting vertical stiffness $c_B = 2c_{B0}$.

$$\Delta F = 2\Delta F_B = c_B \cdot \Delta y = 2c_{B0} \cdot \Delta y \quad . \tag{7.1.5-2}$$

This common mode bearing vibration has been already described in Section 7.1.3, leading to common mode (c.m.) natural frequency

$$f_{B,c.m.} = \frac{1}{2\pi} \cdot \sqrt{\frac{c_B}{m_r}} \qquad (7.1.5\text{-}3)$$

If both bearings vibrate with 180° PHASE SHIFT (differential mode vibration) e.g. in vertical direction due to phase shift of 180° between left and right bearing force $\Delta F_{BL} = -\Delta F_{BR}$, the rotor body is not only oscillating vertically (Fig. 7.1.5-1b), but shows also angular movement around *x*-axis with angle α, which according to $J_x \cdot d^2\varphi / dt^2 = M$ is ruled by the moment of inertia of rotor body around *x*-axis and by the torque $\Delta M = L \cdot \Delta F_B$. The resulting **differential mode natural frequency** (given without proof here)

$$f_{B,d.m.} = \frac{1}{2\pi} \cdot \frac{L}{2} \cdot \sqrt{\frac{c_B}{J_x}} > f_{B,c.m.} \qquad (7.1.5\text{-}4)$$

is usually higher than the common mode natural frequency, if L is big enough.

Conclusions:
In the complete motor system elasticity of bearings and end shields leads to two rigid rotor body vibrations, which may influence (disturb) the balancing process of the complete motor system, if rotational speed f = n coincides with on of these two natural frequencies, leading to resonance. The balancing of the rotor alone on a balancing machine is not influenced by these bearing vibrations, as on the balancing machine the rotor runs in special measuring bearings.

b) Elastic rotor shaft with lumped mass assumption:
The rotor iron stack, consisting of the stacked iron sheets, shows no big stiffness, compared to massive cylindrical rotor body of the same dimensions. So it is mainly the massive rotor shaft (mass m_{sh}), which determines rotor stiffness ($c_{sh} = c_r$). The rotor iron stack (mass m_{stack}) acts mainly as additional mass. Here for simplicity the model of **disc rotor** (thickness l_{Fe} much smaller than diameter d_{ra} and bearing distance L) is considered. This model is very applicable to a one stage steam turbine rotor and was first studied by *de Laval*, thus being called *Laval* rotor. Mass of shaft is added as **lumped mass** to stack mass as total rotor mass $m_r = m_{stack} + m_{sh}$, which is mounted on elastic mass-less shaft (here for simplicity in the middle between both bearings at $z = L/2$). Elasticity of shaft is described by *Young´*s modulus E, which for steel is $E = 212 \cdot 10^9\,\mathrm{N/m^2}$. Shaft circular cross section with diameter d_{sh} resists to bending with area momentum of inertia $I = \pi \cdot d_{sh}^4 / 64$. Shaft length between bearing is bearing distance L (Fig. 7.1.5-2). For simplification we assume rotor disc to be centred between the bearings. At stand still due gravity the shaft is bent with maximum deformation y_M in the middle (Fig. 7.1.5-2)

$$F = m_r \cdot g = c_{sh} \cdot y_M \qquad (7.1.5\text{-}5)$$

with

$$c_{sh} = \frac{48 \cdot E \cdot I}{L^3} \quad . \qquad (7.1.5\text{-}6)$$

Example 7.1.5-1:
Electric motor with 75 kW at 1500/min:
Shaft length / diameter L = 0.7 m, d_{sh} = 80 mm, stack length l_{Fe} = 350 mm,
outer diameter d_{ra} = 190 mm, iron mass density ρ = 7850 kg/m^3:

$m_{sh} = \rho \cdot L \cdot d_{sh}^2 \pi / 4 = 27.6\,\text{kg},\ m_{stack} = \rho \cdot l_{Fe} \cdot (d_{ra}^2 - d_{sh}^2)\pi / 4 = 64.1\,\text{kg},$

$m_r = 27.6 + 64.1 = 91.7\,\text{kg},\ I = \pi \cdot d_{sh}^4 / 64 = 2.01 \cdot 10^{-6}\,\text{m}^4,\ c_{sh} = \frac{48 \cdot E \cdot I}{L^3} = 59.63 \cdot 10^6\,\text{N/m}$

Static rotor bending due to gravity: $y_M = m_r \cdot g / c_{sh} = 15\,\mu\text{m}$

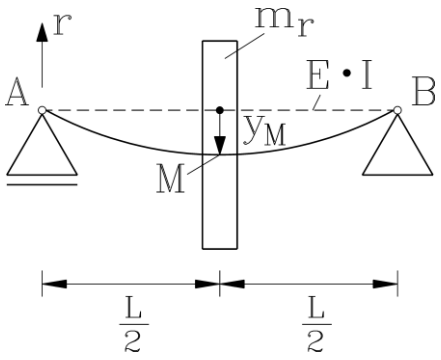

Fig. 7.1.5-2: Disc rotor on elastic shaft (*Laval* rotor)

Natural bending frequency is given by

$$m_r \cdot \ddot{y} + c_{sh} \cdot y = 0 \qquad (7.1.5\text{-}7)$$

with **natural bending frequency**

$$\boxed{f_b = \frac{1}{2\pi} \cdot \sqrt{\frac{c_{sh}}{m_r}}} \quad . \qquad (7.1.5\text{-}8)$$

Conclusions:
For getting stiff rotor the distance between the bearings must be small and the shaft diameter should be big. This and small rotor mass allow increase of rotor bending natural frequency.

Example 7.1.5-2:
Electric motor with 75 kW at 1500/min (Date of Example 7.1.5-1):

$m_r = 91.7\,\text{kg},\ c_{sh} = 59.63 \cdot 10^6\,\text{N/m}$

Natural bending frequency is $f_b = \frac{1}{2\pi} \cdot \sqrt{\frac{c_{sh}}{m_r}} = \frac{1}{2\pi} \cdot \sqrt{\frac{59631953}{91.7}} = \underline{\underline{128.3}}\,\text{Hz}$

At speed $n = f_b = 7700$/min an imbalance will excite big motor vibrations due to resonance. Therefore maximum motor speed should stay below $n_{max} = f_b \cdot 0.7 = 5390$/min.

c) Elastic rotor shaft with distributed mass:
In reality the shaft has to be considered as cylindrical beam of diameter d_{sh} and length L with DISTRIBUTED mass along the beam. Like a vibrating guitar string, this beam has not only one bending natural frequency, but a whole spectrum of natural bending modes, which depend on the elasticity of the bearings. Assuming rigid bearings, where the *x*- and *y*-co-ordinate of the beam is always zero, but allowing the beam to change its inclination also at the bearing´s location, the natural bending frequencies of the beam (with cross section areas *A*) are derived as

$$f_{b,i} = \frac{1}{2\pi} \cdot \left(\frac{i \cdot \pi}{L}\right)^2 \cdot \sqrt{\frac{E \cdot I}{\rho \cdot A}} \quad , \quad i = 1, 2, 3, \ldots \qquad (7.1.5\text{-}9)$$

As the iron stack mass increases the total mass, this considered according to (7.1.5-8) by

$$f_{b,i,corr} = f_{b,i} \cdot \frac{1}{\sqrt{1+\frac{m_{stack}}{m_{sh}}}} \quad , \quad i = 1, 2, 3, ... \tag{7.1.5-10}$$

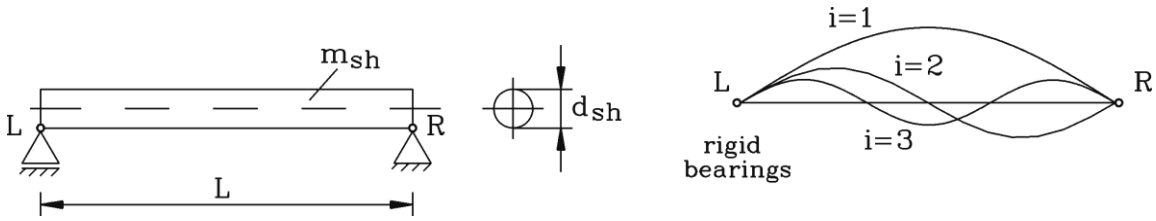

Fig. 7.1.5-3: Model of shaft as cylindrical beam, showing a spectrum of bending natural frequencies, which depend on the influence of bearing stiffness

Example 7.1.5-3:
Electric motor with 75 kW at 1500/min (data of Example 7.1.5-1) :
L = 0.7 m, d_{sh} = 80 mm, ρ = 7850 kg/m^3, $m_{sh} = 27.6\,\text{kg}$, $m_{stack} = 64.1\,\text{kg}$,
$1 + m_{stack}/m_{sh} = 1 + 64.1/27.6 = 3.32$, $A = \pi \cdot d_{sh}^2/4 = 5.03 \cdot 10^{-3}\,\text{m}^2$

i	1	2	3
$f_{b,i,corr}$ / Hz	182	731	1645

Compared with the simplified lumped mass model (7.1.5-6), the more detailed model (7.1.5-10) yields 40% higher first natural bending frequency and in addition also higher frequency eigen-modes.

Bigger motors have rather big distance of bearings L and rather big rotor mass. Hence, to consider influence of machine size on natural bending frequency, we take geometric dimensions $L \sim x, d_{sh} \sim x$ in (7.1.5-9), showing that frequency decreases inverse with increasing frame size: $f_{b,i} \sim 1/x$.

Conclusions:
Calculation of natural bending frequency is rather complicated, as distributed mass and geometry of rotor has to be considered. The stiffening influence of rotor iron stack is also difficult to calculate. Elasticity of bearings may reduce the natural bending frequencies by about 10 % to 20 %. Further, big machines have low natural bending frequency.

d) Influence of "unbalanced magnetic pull" on natural bending frequency:
When the rotor shaft is bent by *y*, this leads to an air gap eccentricity *e* = -*y* . The electric machine air gap is reduced on side by $\delta - e$ and increased on the other side by $\delta + e$. Thus radial magnetic flux density, which is excited by m.m.f. in air gap V_δ, in case of machines with pole numbers $2p \geq 4$ is increased on side by $B_{\delta+} = \mu_0 \cdot V_\delta / (\delta - e)$ and reduced on the opposite side by $B_{\delta-} = \mu_0 \cdot V_\delta / (\delta + e)$. Thus radial magnetic pull per unit rotor surface $A_r = 2p \cdot \tau_p \cdot l_{Fe}$ with $B_\delta = \mu_0 \cdot V_\delta / \delta$ as air gap flux density amplitude of non-eccentric rotor

$$f_{n+} = \frac{B_{\delta+}^2}{2\mu_0} > f_{n-} = \frac{B_{\delta-}^2}{2\mu_0} \tag{7.1.5-11}$$

is no longer in equilibrium, but residual ("unbalanced") magnetic pull in direction of decreased air gap remains (formula given without proof):

$$F_M = (f_{n+} - f_{n-}) \cdot A_r = \frac{p \cdot \tau_p \cdot l_{Fe}}{2\mu_0} \cdot B_\delta^2 \cdot \frac{e}{\delta} \quad , \quad 2p \geq 4 \tag{7.1.5-12}$$

For **two-pole machines** this unbalanced magnetic pull is only 50%.
Note: At zero eccentricity $e = 0$ this residual pull is also zero.

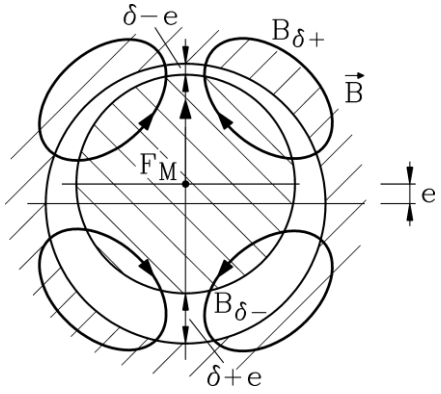

Fig. 7.1.5-4: "Unbalanced magnetic pull" F_M in four pole motor due to air gap eccentricity e

This residual radial magnetic force tends to decrease the reduced air gap further. Comparing with the elastic bending of the shaft, where a bending by value y increases elastic force $F_{c_{sh}} = c_{sh} \cdot y$, acting against the bending force, the unbalanced magnetic pull acts in direction of bending force, thus opposite to elastic force:

$$F_M = -c_M \cdot y \quad . \tag{7.1.5-13}$$

Considering $y = -e$, the "magnetic stiffness"

$$c_M = \frac{p \cdot \tau_p \cdot l_{Fe}}{2\mu_0} \cdot B_\delta^2 \cdot \frac{1}{\delta} \tag{7.1.5-14}$$

has to be considered in the model of elastic rotor. It **reduces the resulting stiffness** by

$$c_{res} = c_{sh} - c_M \quad , \tag{7.1.5-15}$$

leading to decrease of natural bending frequency by

$$\boxed{f_{b,M} = \frac{1}{2\pi} \cdot \sqrt{\frac{c_{sh} - c_M}{m_r}} = f_b \cdot \sqrt{1 - \frac{c_M}{c_{sh}}}} \quad . \tag{7.1.5-16}$$

Example 7.1.5-4:
4-pole electric motor with 75 kW at 1500/min (data of example 7.1.5-3):
L = 0.7 m, d_{sh} = 80 mm, l_{Fe} = 350 mm, d_{ra} = 190 mm, $m_r = 91.7\,\text{kg}$, air gap flux density amplitude B_δ = 0.9 T, air gap δ = 1.0 mm, pole pitch: $\tau_p = 149\,\text{mm}$

Rotor gravity force: $m_r \cdot g = 900\,\mathrm{N}$
Unbalanced magnetic pull at 10% eccentricity: $e/\delta = 0.1$:

$$F_M = \frac{p \cdot \tau_p \cdot l_{Fe}}{2\mu_0} \cdot B_\delta^2 \cdot \frac{e}{\delta} = \frac{2 \cdot 0.149 \cdot 0.35}{2 \cdot 4\pi \cdot 10^{-7}} \cdot 0.9^2 \cdot 0.1 = \underline{\underline{3360}}\,\mathrm{N}$$

Depending on air gap eccentricity, the unbalanced magnetic pull can reach considerable values (here: 225 % of rotor gravity force).

Calculated first natural bending frequency without influence of magnetic pull: $f_{b1} = 183\,\mathrm{Hz}$:
equivalent shaft stiffness: $c_{sh} = (2\pi f_{b1})^2 \cdot m_r = 121.4 \cdot 10^6\,\mathrm{N/m}$,
magnetic stiffness: $c_M = \frac{p \cdot \tau_p \cdot l_{Fe}}{2\mu_0} \cdot B_\delta^2 \cdot \frac{1}{\delta} = 33.6 \cdot 10^6\,\mathrm{N/m}$
Calculated first natural bending frequency with influence of unbalanced magnetic pull:
$f_{b1,M} = f_{b1} \cdot \sqrt{1 - c_M / c_{sh}} = 183 \cdot \sqrt{1 - 33.6/121.4} = \underline{\underline{155.6}}\,\mathrm{Hz}$:

Conclusions:
Unbalanced magnetic pull leads to a considerable decrease of natural bending frequency by about 10% ... 20%, depending on utilization of magnetic circuit.

7.1.6 Balancing of elastic rotors

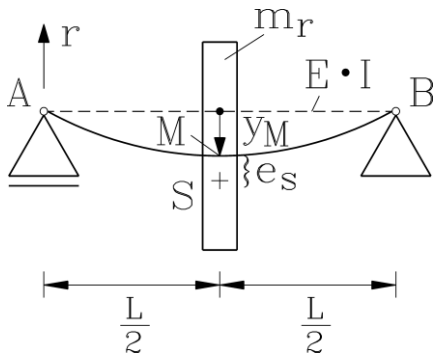

Fig. 7.1.6-1: Static imbalance due to dislocation of centre of gravity *S* by e_S from rotational axis. Additional dislocation of centre of rotation from geometrical axis of unbent shaft (here: Example of disc rotor on elastic shaft (*Laval* rotor))

We assume static imbalance due to dislocation of centre of gravity *S* by e_S from rotational axis (Fig. 7.1.6-1). Neglecting the bending due to gravity, we here consider only bending due to centrifugal force caused by imbalance, which causes in *y*-direction additional dislocation y_M of centre of rotation *M* from geometrical axis of unbent shaft. In *x*-direction dislocation x_M occurs. With resulting radial dislocation $r_M = \sqrt{x_M^2 + y_M^2}$ due to bending the centre of gravity is displaced from geometrical axis by $r_S = e_S + r_M$, causing centrifugal force

$$F_S = m_r \cdot (e_S + r_M) \cdot \Omega_m^2 = m_r \cdot r_S \cdot \Omega_m^2 \quad . \qquad (7.1.6\text{-}1)$$

The shaft bends until equilibrium between centrifugal force and elastic force is reached,

$$F_S = F_{c_{sh}} \quad \Rightarrow \quad m_r \cdot (e_S + r_M) \cdot \Omega_m^2 = c_{sh} \cdot r_M \quad , \qquad (7.1.6\text{-}2)$$

yielding for the displacement r_M of centre of rotation *M* from geometrical axis in dependence of speed

$$r_M = e_S \cdot \frac{\Omega_m^2}{\omega_b^2 - \Omega_m^2} \quad , \qquad \omega_b = 2\pi \cdot f_b \tag{7.1.6-3}$$

and for the displacement r_S of centre of gravity *S* from geometrical axis in dependence of speed (Fig. 7.1.6-2)

$$\boxed{r_S = e_S \cdot \frac{\omega_b^2}{\omega_b^2 - \Omega_m^2}} \quad . \tag{7.1.6-4}$$

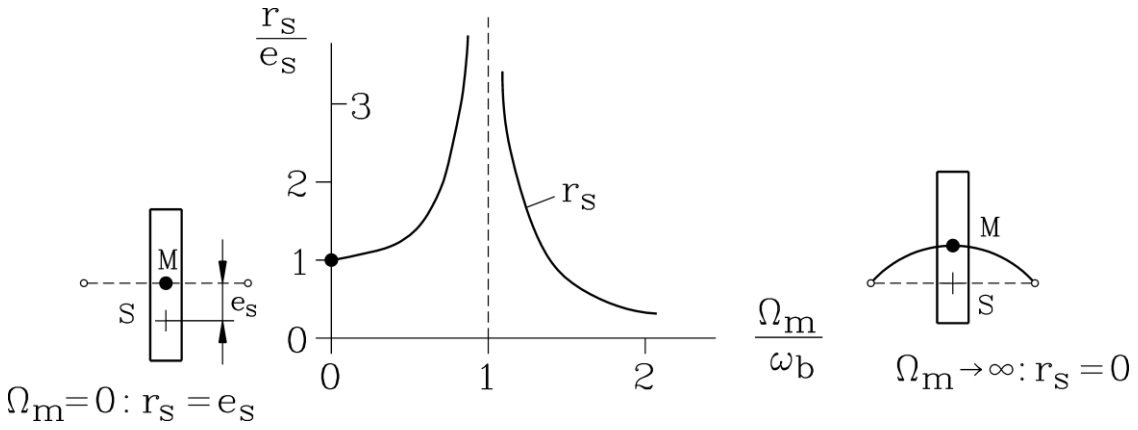

Fig. 7.1.6-2: Displacement r_S of centre of gravity *S* from geometrical axis in dependence of speed

After passing through the resonance region, the centre of gravity is centring itself on the geometrical axis at high speed ($r_S \to 0$); hence the centrifugal force will vanish at high speed. Centrifugal force is depending not only on U_S and Ω_m^2, but also on the ratio of Ω_m / ω_b, so rigid body balancing is not possible any longer.

$$\boxed{F_S = m_r \cdot e_S \cdot \frac{\omega_b^2}{\omega_b^2 - \Omega_m^2} \cdot \Omega_m^2 = U_S \cdot \frac{1}{1-(\Omega_m / \omega_b)^2} \cdot \Omega_m^2} \tag{7.1.6-5}$$

In order to minimize the increase of centrifugal force and the related bearing forces

$$\begin{aligned} \vec{F}_{A,x\sim} &= \vec{F}_{B,x\sim} = F_S / 2 \cdot \cos(\Omega_m t) \\ \vec{F}_{A,y\sim} &= \vec{F}_{B,y\sim} = F_S / 2 \cdot \sin(\Omega_m t) \end{aligned} \tag{7.1.6-6}$$

near resonance $\Omega_m \approx \omega_b$, **special balancing techniques** for elastic rotors have been developed. In a third plane additional balancing masses are fixed. This third plane should be located at the rotor near the location of maximum rotor bending. The centrifugal force of this added imbalance shall act opposite to the centrifugal force of the bent shaft.

Small and medium sized motors are operated even with high speed application usually below first natural bending frequency. So the rigid body balancing is sufficient. But bigger motors

have their first natural bending frequency already **below** their rated speed, so **elastic balancing** is necessary. Big 2-pole turbo generators for steam power plants with bearing distances L of several meters, being operated at 3000/min = 50 Hz, have typically 2 or 3 natural bending frequencies below 50 Hz. Elastic balancing needs for each natural bending frequency, which is below maximum machine operating speed, an additional balancing plane to fix further balancing masses. The centrifugal forces of these added imbalances shall counter-act to the bending modes of the rotor at each of the natural bending frequencies.

Example 7.1.6-1:
a) 2-pole standard induction motor, 50 Hz, 500 kW:
1^{st} natural bending frequency at f_{b1} = 35 Hz.
Elastic balancing with 3 balancing planes is necessary.
b) 2-pole large synchronous turbo generator, 50 Hz, 1000 MW (power plant *Lippendorf, Germany*): 3 natural bending frequencies lie in the frequency range 5 ... 40 Hz:
Elastic balancing with 5 balancing planes is necessary.